Climate Services 30 (2023) 100363

Contents lists available at ScienceDirect

Climate Services

journal homepage: www.elsevier.com/locate/cliser

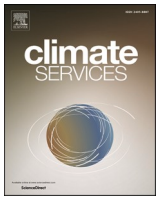

Original research article

The probability of unprecedented high rainfall in wine regions of northern Portugal

Michael G. Sanderson [a,*], Marta Teixeira [b], Natacha Fontes [b], Sara Silva [b], António Graça [b]

[a] Met Office, Fitzroy Road, Exeter EX1 3PB, UK
[b] Sogrape Vinhos, S.A., Aldeia Nova, 4430-809 Avintes, Portugal

ARTICLE INFO

Keywords:
Extreme rainfall
Northern Portugal
Decadal forecasts
Extreme value analysis
Viticulture

ABSTRACT

Climate is arguably one of the most important factors determining the quality of wine from any given grapevine variety. This study focuses on three wine-growing regions in northern Portugal: Vinho Verde, Trás-os-Montes and Douro, the latter coinciding with Porto. High rainfall during late spring (April to June) can promote growth of the vines but increases the risk of fungal disease. High rainfall during harvest time (August to October) also bears the potential for severe operational disruption and heavy economic losses. The probability of unprecedented rainfall totals in spring and the harvest season over wine-growing regions of northern Portugal has been assessed. A large ensemble of initialised climate model simulations is analysed, and the probability of unprecedented rainfall in each season is quantified. Seasonal rainfall totals considerably higher than any observed are possible in the current climate. An unprecedented rainfall event in either season could occur with a probability between 0.01 and 0.05 in the present climate. Extreme value analysis was applied to rainfall totals from observations and the model ensemble, and the return periods of known extreme rainfall events are calculated. Similar probabilities for unprecedented rainfall totals were calculated. A year similar to 1993, when both seasons were exceptionally wet, would be expected to occur, on average, just once in the next 70–80 years in the current climate. These results could inform the requirements for improved vineyard management and resilience, such as design of drainage channels, access roads and terraces.

Practical implications

In Portugal, vitiviniculture is a key socioeconomic sector. Many vineyards in northern Portugal, especially those planted along the Douro River, are situated on the steep slopes of the valley sides. Very high rainfall events lead to erosion of the soils, increased disease prevalence and higher production costs while reducing grape yields. They may also cause landslides and the collapse of terrace banks both endangering human lives and incurring heavy repair costs for both private and public infrastructure (Santos et al., 2015). Assessments of projections of climate over northern Portugal suggest the region would become warmer and drier in the future. Changes in the amount of extreme precipitation are less clear, with both increases and decreases reported by different studies (Martins et al., 2021). Nevertheless, extreme or unprecedented rainfall events could still occur in the next few decades, and the contribution of extreme precipitation to rainfall totals could also increase.

The added value of seasonal and decadal forecasts in the wine sector is becoming increasingly recognised. Santos et al. (2020) developed a predictive model of Port wine production in the Porto and Douro DOC region driven by seasonal forecasts. This study is an important first step in the development of a potential climate service for wine growers. Unprecedented rainfall events in either spring (here, April to June) or harvest time (August to October) have a probability between 0.01 and 0.05 in the present climate. These events are therefore expected to occur, on average, once in the next 20–100 years. However, they could occur more than once. The response of wine growers to this result would depend on their risk appetite, and the costs of adaptation compared with potential losses. The most immediate impact is a science-based input for dimensioning drainage networks in slope vineyards, as well as the design of terraces and service roads with adapted inclination both on the longitudinal and transversal axes. This information, coupled together with very-high resolution mapping of surface and subsurface water flows, is critical to achieve

* Corresponding author.
E-mail address: michael.sanderson@metoffice.gov.uk (M.G. Sanderson).

https://doi.org/10.1016/j.cliser.2023.100363
Received 18 April 2022; Received in revised form 4 January 2023; Accepted 25 January 2023
Available online 10 February 2023

vineyard designs with higher safety performance (Alves et al., 2021; Fernandes et al., 2017; Faria et al., 2017).

The next practical step would be to assess the predictive skill of unprecedented rainfall totals in operational seasonal forecasts from different modelling centres. If these forecasts have sufficient skill, an operational service could then be developed for wine growers in northern Portugal to provide the risk of an unprecedented rainfall event in the following months. The availability of such an operational service would provide farmers, municipal and wine region authorities with a base for respectively managing and enforcing measures to reduce resistance to downslope water flow and to plan and budget for rapid response in the event of landslides. Scheduling of major terraforming works in vineyard plantation and restructuring, especially when funded from public sources (VITIS program under the Common Market Organization framework), would also greatly benefit from the availability of such a service, which would identify periods when such works should be avoided because of high rainfall risks.

This study has demonstrated the successful application of a large ensemble method to the agriculture sector. This approach could be applied to other climatic variables and assess the probability of other hazards over northern Portugal such as hot summers and droughts.

Data availability

A Data Sources section showing links to all the data used is at the end of the supplemental material.

1. Introduction

Vineyards have existed in the Douro region of northern Portugal for 2,000 years. The main product from the mid-eighteenth century, Port wine, is world famous for its quality. The importance of viticulture in the Alto Douro region was recognised in 2001 when this area was granted UNESCO World Heritage status for its living and evolving landscape (Fonseca and Rebelo, 2010). Wine making continues to be of key socioeconomic importance in Portugal. In 2021, Portugal was the 10th largest wine exporter (by volume) and 10th largest producer worldwide (OIV, 2022a). The focus of the present study is northern Portugal, defined as the region between 8°50′W and 6°30′W, and 40°30′N to 42°0′N (Fig. 1, rectangular area). This area includes the wine-growing regions of Vinho Verde, Trás-os-Montes and Porto and Douro geographical indications (GI), whose borders are shown in Fig. 1.

Northern Portugal has a typical Mediterranean climate, with warm dry summers and mild and wet autumns and winters. Rainfall totals in this region vary considerably, with over 2200 mm yr^{-1} in the west to just 600 mm yr^{-1} in the east (Cunha et al., 2011). Climate, together with soil, plant material and cultural practices, is arguably-one of the most important factors determining the quality of wine from any given grapevine variety and an important element of the concept of terroir (Gladstones, 2011; Jones and Alves, 2012). Terroir refers to "an area in which collective knowledge of the interactions between the physical and biological environment (soil, topography, climate, landscape characteristics and biodiversity features) and vitivinicultural practices develops, providing distinctive wine characteristics" (OIV, 2010). A large diversity of terroirs are present in northern Portugal owing to the different types of soils, climatic variations between vineyards, viticultural management and grapevine varieties.

Heavy rainfall can have a variety of impacts on vineyards. Those in the Douro valley are often sited on terraces on steep slopes, and so the soils are prone to erosion by heavy rainfall. For example, 80 mm of rain fell on the 28th May 2018 in Pinhão in the Douro Valley (Millar, 2018), damaging terraces and washing away soils. Some vineyards suffered losses as high as 80 %. Winter rainfall is normally welcome, because it

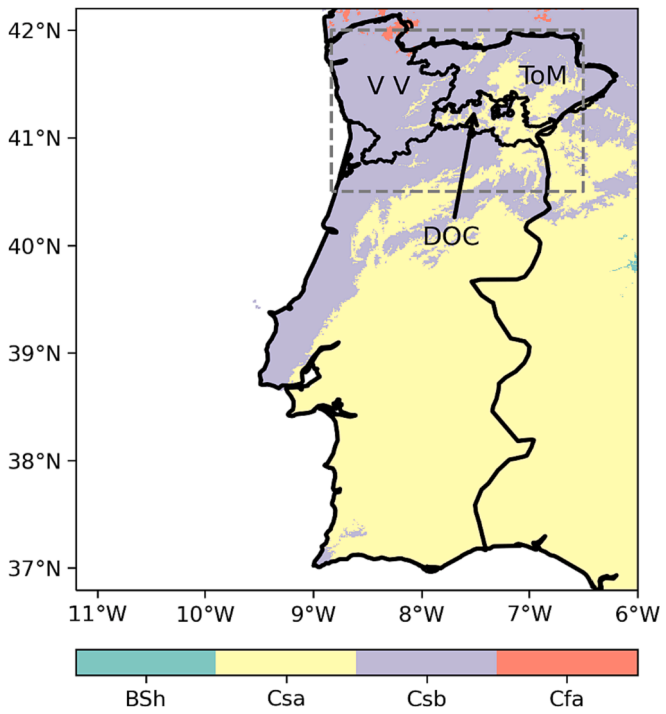

Fig. 1. Map of Portugal showing the Koeppen climate zones: BSh – Arid, steppe, hot; Csa – Temperate, dry hot summer; Csb – Temperate, dry warm summer; Cfa – Temperate, without dry season, hot summer. The Koeppen climate data were created by Cui et al. (2021a,b). The outlines of three wine growing regions Vinho Verde (VV), Trás-os-Montes (ToM) and Porto and Douro DOC are also shown. The study area (8°50′W to 6°30′W, and 40°30′N to 42°0′N) is indicated by the dashed grey lines.

allows the replenishment of the soil water reserves ensuring an even vegetative development. High rainfall during late spring (April to June) may increase the risk of fungal disease and disrupt vine phenology, namely blossom and fruit set, which occur during this period. This was the case in the Douro valley in 1983, 1988, 1993, 2008 and 2016, when higher than average late spring rainfall increased the risk of fungal disease, especially downy mildew (*Plasmopara viticola*), among others. There was a need to permanently monitor the vines and apply the necessary phytosanitary treatments while managing canopy development that, because of high water availability, grew excessively (Graça A., personal communication; ADVID, 2016). This resulted in higher costs of production from extra labour, farming machinery and plant protection products associated with downy mildew control. Some level of crop loss was notwithstanding unavoidable, as farmers were not prepared for that level of disease pressure.

Although studies of climate projections suggest an overall drying trend in Portugal, the contribution of extreme and unprecedented rainfall events to overall rainfall totals could increase in the future (Martins et al., 2021). In this study, the probability of unprecedented rainfall totals over northern Portugal is assessed in two critical periods of vine phenology (Fraga et al., 2017): budburst and flowering (April to June) and grape maturation and harvest (August to October).

One major issue for assessing these probabilities is the relatively short period of observations available. It is difficult to assess the probability of extreme events from a short data series, as the number of events may be under-sampled. Two approaches will be used to estimate the probability of unprecedented rainfall totals over northern Portugal. First, the empirical probability of unprecedented rainfall is estimated using a large ensemble of decadal climate hindcasts. This ensemble provides considerably more simulations of the recent climate than are available from observations (Thompson et al., 2019). The decadal forecast model, if it reproduces observed climate variability, is capable

of sampling more extreme rainfall events, allowing the identification of unprecedented rainfall events and assessing their likelihood in the real world (Thompson et al., 2017; Kelder et al., 2020). Secondly, extreme value analysis (EVA; Coles, 2001) will be used to calculate the probabilities of unprecedented rainfall totals in the observations and decadal hindcasts.

2. Materials and methods

The risk of unprecedented rainfall totals over northern Portugal is assessed in the two critical periods described above: budburst and flowering (April to June) and grape maturation and harvest (August to October). These two periods will be referred to as spring and harvest time throughout this paper. Links to the data used are provided in the "Data Sources" Section in the Supplemental material.

2.1. Decadal hindcasts

Simulated seasonal rainfall totals were taken from the Met Office's decadal climate prediction system DePreSys3 (Dunstone et al., 2016). These simulations are based on the HadGEM3 GC2 global climate model (Williams et al., 2015) and are integrated at a horizontal resolution of 0.83° (60 km) in the atmosphere and 0.25° in the ocean. The model is initialised with atmospheric, oceanic, and sea-ice observational data and current anthropogenic and natural forcings, so that the simulations are representative of current real-world climate. The hindcasts used here were produced from 1980 to 2017, when satellite data are available for model initialisation. The hindcasts begin on the 1st November of each year, corresponding to the start of each viticultural campaign. Forty ensemble members are available for each year, providing 1520 simulations (38 years × 40 members) of spring and harvest time rainfall totals. The use of initialised climate predictions reduces model biases compared with uninitialized transient simulations of the past climate (Thompson et al., 2017). The five- and nine-month lead times allows the forecasts from the ensemble members to diverge, producing a wide range of plausible extreme rainfall events, some of which will not have been observed (Kent et al., 2017). Rainfall totals for spring (April to June) and harvest time (August to October) were calculated for northern Portugal (Fig. 1).

Extreme rainfall events over northern Portugal can originate from weather fronts and localised convective storms. Daily rainfall series for northern Portugal were calculated for years and seasons with exceptionally high rainfall totals (e.g., spring 2016; see Figs. 2 and S2). An examination of analysis charts produced by the Met Office on days with very high rainfall totals showed that many of these events originated from slow-moving weather fronts lying over northern Portugal (Fig. S2). DePreSys3 can resolve these fronts, giving confidence in its ability to simulate realistic rainfall totals. Other studies have shown that high rainfall totals in the Douro valley originated from frontal activity associated with Atlantic cyclonic systems (Santos et al., 2015; Alcoforado et al., 2021). Hénin et al. (2021) and Owen et al. (2021) showed that cyclones and fronts are the most common drivers of concurrent precipitation and wind extremes over northern Portugal and elsewhere in Europe.

2.2. Precipitation observations

Three different gridded datasets (Table 1) were used to calculate precipitation totals over northern Portugal and evaluate the DePreSys3 hindcasts. Two datasets, Iberia01 (Herrera et al., 2019a,b) and E-OBS (Cornes et al.,2018) include daily precipitation totals at 0.1° spatial resolution (about 11 km). These two datasets were created via interpolation of surface rain gauge data, although the methods used were different. Iberia01 was derived from nearly 3500 gauges, but only 128 gauges (in the year 2000) were available for E-OBS. A comparison between Iberia01 and an older version of E-OBS (17e) by Herrera et al. (2019a) showed that E-OBS underestimated mean precipitation by 15 %, and extreme rainfall totals by a larger margin. The third dataset, the Climate Hazards group Infrared Precipitation with Stations (CHIRPS), is a combination of global Cold Cloud Duration (CCD) rainfall estimates derived from satellite observations and surface rain gauge data (Funk et al., 2015). During the study period (1980–2017), the number of rain gauges in Portugal and Spain declined (Cornes et al., 2018; Herrera et al., 2019a), meaning any trends calculated from the Iberia01 and E-OBS datasets should be treated with caution. Between 2009 and 2014 there were very few precipitation stations in northern Portugal (Herrera et al., 2019a), which will affect the estimated rainfall totals in all three datasets.

Table 1
Gridded daily rainfall datasets used in this study. The resolutions in km are approximate.

Dataset Name	Version	Resolution	Data Period	Reference
Iberia01	1.0	0.1° (11 km)	1971–2015	Herrera et al. (2019a, b)
E-OBS	23.1e	0.1° (11 km)	1950–2020	Cornes et al. (2018)
CHIRPS	2.0	0.05° (6 km)	1981–2020	Funk et al. (2015)

Time series of rainfall totals for spring and harvest time calculated from CHIRPS, Iberia01 and E-OBS for northern Portugal are shown in Fig. S1. Considerable variation between years is evident and the years with very high precipitation totals are the same in all three datasets, although the absolute amounts differ. Generally, the lowest precipitation totals are seen in E-OBS, particularly in spring (Fig. S1, upper panel). Some differences in the temporal behaviour between the three datasets are also evident from 2011 during harvest time (Fig. S1, lower panel).

2.3. Data analysis, visualisation, and statistics

The interior of northern Portugal is characterised by considerable orographic variation, with mountains over 1200 m high separated by deep valleys (https://en-gb.topographic-map.com/maps/lp72/Portugal/). Precipitation variations between catchments in this area cannot be resolved by a global model with a resolution of 60 km. Therefore, the precipitation time series presented in this study are spatial averages over the area indicated by the dashed grey lines in Fig. 1.

The absolute magnitude of extreme events is useful for design purposes. Extreme rainfall amounts can be estimated for a given return period using extreme value theory (Coles, 2001). A return period of 10 years means an event of a given magnitude would be expected to occur, on average, once every 10 years. An alternative interpretation is the event would have a probability of 1/10 of occurring in any given year. Extreme value analysis allows the calculation of return periods and probabilities of events that are more extreme than any observed. It therefore provides a useful complementary approach for estimating the probabilities of unprecedented rainfall events. The interest here is in very high rainfall totals above a threshold (i.e., the highest observed rainfall totals). A Generalised Pareto (GP) distribution is suitable for fitting to excesses over a high threshold (Coles, 2001). The distribution function of the GP is:

$$H(x) = 1 - \left[1 + \xi\left(\frac{x-u}{\sigma_u}\right)\right]^{-1/\xi}$$

where u is a suitable threshold and x represents precipitation totals greater than u (i.e., $x > u$). The symbols σ_u and ξ are the scale and shape parameters respectively, which determine the rate of change of the extremes with increasing return period. The return levels of given rainfall amounts, and the corresponding probabilities of precipitation exceeding a given amount (p) can be obtained by setting H(x) equal to 1 – p and

inverting the equation above (Coles, 2001; Gilleland and Katz, 2016). The GP distribution was fitted to the observed and modelled rainfall data using R software (https://www.R-project.org), specifically the package "extRemes" version 2.0 (Gilleland and Katz, 2016). The scale (σ_u) and shape (ξ) parameters for a given threshold (u) were found using maximum likelihood estimation. The thresholds for each season were identified from inspection of mean residual life (MRL) and threshold choice (TC) plots (Coles, 2001).

All other data analysis and visualisation was performed using the Python language (https://www.python.org) and associated packages. Correlations were assessed using Pearson and Spearman correlation coefficients. Linear trends were calculated using a method that is robust to outliers (Press et al. (1992), pp.694–700).

3. Results

3.1. Impact of heavy rainfall on wine production and quality

In Fig. 2, the total grape must production (red line) from selected vineyards in the upper Douro valley is clearly lower in those years with very high spring rainfall (blue line; see Section 2.2 and Fig. S1), especially 1988, 1993 and 1998. Additionally, the numbers of phytosanitary treatments (solid circles) were also larger in years with high spring rainfall. For example, in 1988, seven treatments were needed, whereas only four or five were applied in 1987 and 1989. In 1993 and 1994, five treatments were required, but in the years either side only one or two treatments were applied. The highest number of treatments was ten in 2016, as a consequence of the very high rainfall during winter (not shown) and spring.

Vineyard management practices have modified must production and lessened the impact of heavy rainfall during spring in the data shown in Fig. 2. Modern viticulture technologies started to be adopted in the late 1980s which matured by the end of the 20th century. The effect is illustrated by the quasi-halving of the standard deviation in production from before the year 2000 (±32.7 Ml) to after 2000 (±17.4 Ml), while average production grew by 11 %. These improvements came from greater technical control of the impact of high spring rainfall. From 2000, integrated pest management strategies were employed and improved disease bioclimatic models had been developed to determine when protective sprayings would be most effective. These measures helped to avoid the extreme deleterious effects of fungal infections seen in earlier years, although some losses were unavoidable.

Other climatic factors moderate the effects of heavy spring rainfall. In 1983 and 2000, lower temperatures in early spring, corresponding to the start of the vine growth cycle, delayed budbreak and vegetation growth. The high levels of rain in these two years also occurred in early spring which reduced the impact on overall must production. However, in 1988, 1993 and 1998, most of the heavy rainfall occurred towards the end of spring, promoting fungal infection of inflorescences and leading to poor fruit set, thus further decreasing must production.

Grape maturation in the Douro region usually starts in mid to late July. The harvest date varies according to each variety, from late August well into September and even October for vineyards at higher altitudes (above 400 m). Heavy rain during harvest time (August to October; Fig. S1) can result in a reduction in the quality of the grapes, by lowering their sugar, acid, flavour and colour values via dilution phenomena. Grape acidity and potential alcohol levels are shown in Fig. 3 for a vineyard in the upper Douro valley. The impacts of the delayed maturity in harvest time of 1993, the wettest year on record in the period analysed, can be seen clearly. In the upper panel, titratable acidity is elevated in this year and the range of values is notably larger than other years. The pH values are also lower in 1993 than other years.

In the lower panel of Fig. 3, the potential alcohol levels in 1993 are significantly reduced. Similar features are present in data from other vineyards in the upper Douro region (not shown). Zhu et al. (2020) found that rainfall near flowering time had a negative effect on berry weight of vines in an area of New Zealand, but no discernible impact of either spring or harvest time rainfall on berry weights was found in the present study. Heavy rain during harvest time can also promote outbreaks of fungal rot (*Botrytis cinerea*) and reduce final yields. It can also disrupt harvest operations, making it more difficult for both labourers and machinery to pick and transport grapes to the winery, further delaying picking which contributes to economic loss much in the way of a damaging feedback loop.

3.2. Hindcast evaluation

An evaluation of the DePreSys3 hindcasts is needed before the probabilities of unprecedented rainfall totals can be calculated. The rainfall totals from Iberia01, CHIRPS and E-OBS were aggregated to the

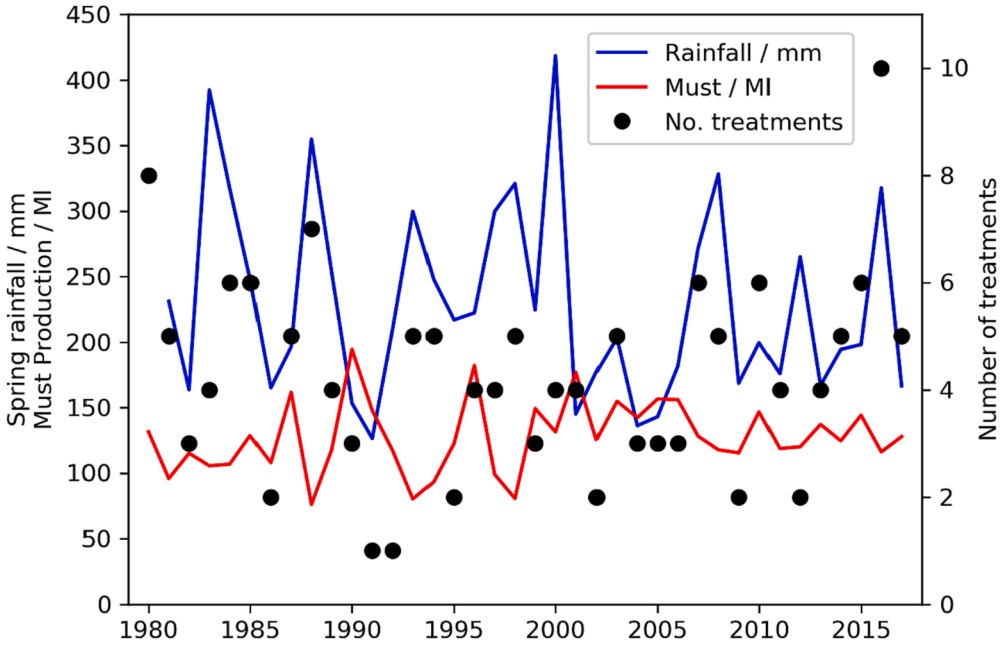

Fig. 2. Total spring (April-June) rainfall over northern Portugal (mm, blue line). Very high rainfall totals are seen in 1983, 1988, 1993, 2008 and 2016. Also shown are total grape must production (millions of litres (Ml), red line) and numbers of phytosanitary treatments recommended to control mildew and other fungal infestations (solid circles). The must production and numbers of phytosanitary treatments were compiled by Sogrape Vinhos from data obtained from official sources in the upper Douro valley: production data from Instituto dos Vinhos do Douro e Porto; recommended treatments from Estação de Avisos do Douro – SNAA/DRAP-N/DGAV (structures within the Portuguese Ministry of Agriculture) and ADVID, a private technical association (https://www.advid.pt). The rainfall totals were calculated from version 2.0 of the CHIRPS dataset (Funk et al., 2015). Northern Portugal is defined as the rectangular region in Fig. 1. (For interpretation of the references to colour in this figure legend, the reader is referred to the web version of this article.)

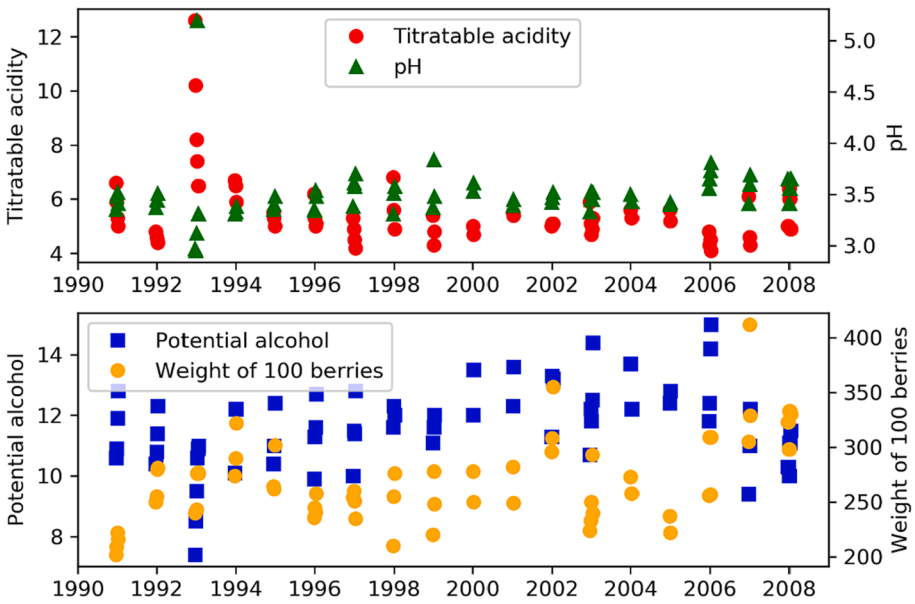

Fig. 3. Selected maturation information for a vineyard planted with *Tinta Barroca*, located at coordinates 41°10′42.4″N, 7°35′05.0″W. The titratable acidity is expressed as grams of tartaric acid per 100 ml. Potential alcohol has units of % volume. The weight of 100 berries is in grams.

resolution of DePreSys3 using an area-weighted method. First, modelled and observed rainfall climatologies for each season over Portugal and Spain are compared (Section 3.2.1). The dependence of the hindcast rainfall totals on the initial conditions and the independence of the individual hindcast ensemble members is assessed in Section 3.2.2. A strong dependence on the initial conditions implies predictability but could moderate the numbers of extreme rainfall events simulated. If the hindcast ensemble members are correlated, the effective ensemble size (and hence true number of extreme seasonal rainfall totals) would be reduced (Kelder et al., 2022). The fidelity of the hindcast ensemble is further examined in Section 3.2.3, where the ability of the hindcast to simulate realistic extreme rainfall events is assessed.

3.2.1. *Comparison of modelled and observed rainfall totals*

Maps showing averaged seasonal rainfall totals from DePreSys3, Iberia01, CHIRPS and E-OBS over the Iberian Peninsula for spring and harvest time are shown in Fig. 4. Rainfall totals are highest over northern Portugal and the north coast of Spain. Rainfall totals decline from north to south in Portugal, and from west to east across Spain, reaching a minimum in the south-east of the country (Cunha et al., 2011). DePreSys3 reproduces the large-scale rainfall patterns seen in the three observed datasets in both seasons. E–OBS has smaller rainfall totals over northern Portugal and Spain than Iberia01 and CHIRPS in spring (Fig. 4, upper panels). During harvest time, rainfall totals are generally lower than those in spring in all datasets. DePreSys3 and E-OBS have a dry bias over northern Portugal and Spain compared with CHIRPS and Iberia01 (Fig. 4, lower panels).

3.2.2. *Independence of ensemble members*

Independence of the ensemble members is important in the present study. Predictability on seasonal timescales is possible via slow fluctuations of components of the Earth system, such as sea-surface temperatures, which can influence patterns in the weather (Dunstone et al., 2016). The hindcasts could have a conditional bias originating from the initial state of these slowly varying components (Kelder et al., 2020). This bias could result in larger or smaller numbers of extreme precipitation events over northern Portugal.

The independence of the hindcast ensemble members was tested in two ways. First, the temporal correlations between the hindcast ensemble mean rainfall totals and rainfall totals from each of the observed datasets were calculated for each season. If the ensemble mean is correlated with the observations, then this implies predictability. The modelled rainfall extremes would be tied to the initial conditions, which could mean a full range of possible climatic states would not be sampled. For spring (April–June), the Pearson's correlation coefficients between the modelled and observed rainfall totals were less than or equal to 0.12 for all three observed datasets (Table 2). The corresponding p-values were$>$0.46, indicating no correlation. The correlation coefficients for harvest time (August to October) rainfall were larger, up to 0.41. The corresponding p-values were smaller (less than 0.1), and that for E-OBS equals 0.01 indicating a strong correlation (Table 2). The hindcasts for spring are therefore independent of the initial conditions, whereas the hindcasts for harvest time represent events that follow the slowly evolving climatic state.

Secondly, the degree of dependence among ensemble members is assessed following the method of Kelder et al. (2020), which is based on the idea of how well a model predicts itself (Dunstone et al., 2016). A pairwise correlation test is applied to identify any dependence between individual ensemble members. There are 780 parings for a 40-member ensemble for each season studied. The precipitation totals from each member are converted to standardised anomalies by subtracting the mean and then dividing by the standard deviation. The Spearman rank correlation coefficient is calculated for each paring using the standardised anomalies. Boxplot statistics (median, interquartile range and the whiskers) were calculated from the 780 correlation coefficients (Fig. 5). The correlation coefficients range from −0.47 to + 0.45. A wide range in values of the correlation coefficient is expected, owing to the large number of tests. The medians are close to zero in both seasons.

Given the large number of correlation tests, a proportion would be expected to be significant by chance. A permutation test is used to estimate the confidence intervals of the boxplot statistics and avoid false detection of significant correlations between the hindcast ensemble members (Kelder et al., 2020). The hindcast data for each season were resampled 1000 times without replacement and the procedure in the previous paragraph was repeated to produce 1000 sets of boxplot statistics. If the ensemble members are truly independent, resampling and recalculating the correlations should produce similar values of the boxplot statistics. The 95 % confidence intervals in the median, interquartile range and whiskers were calculated from the 1000 samples and are shown as grey shaded areas in Fig. 5. The median, interquartile

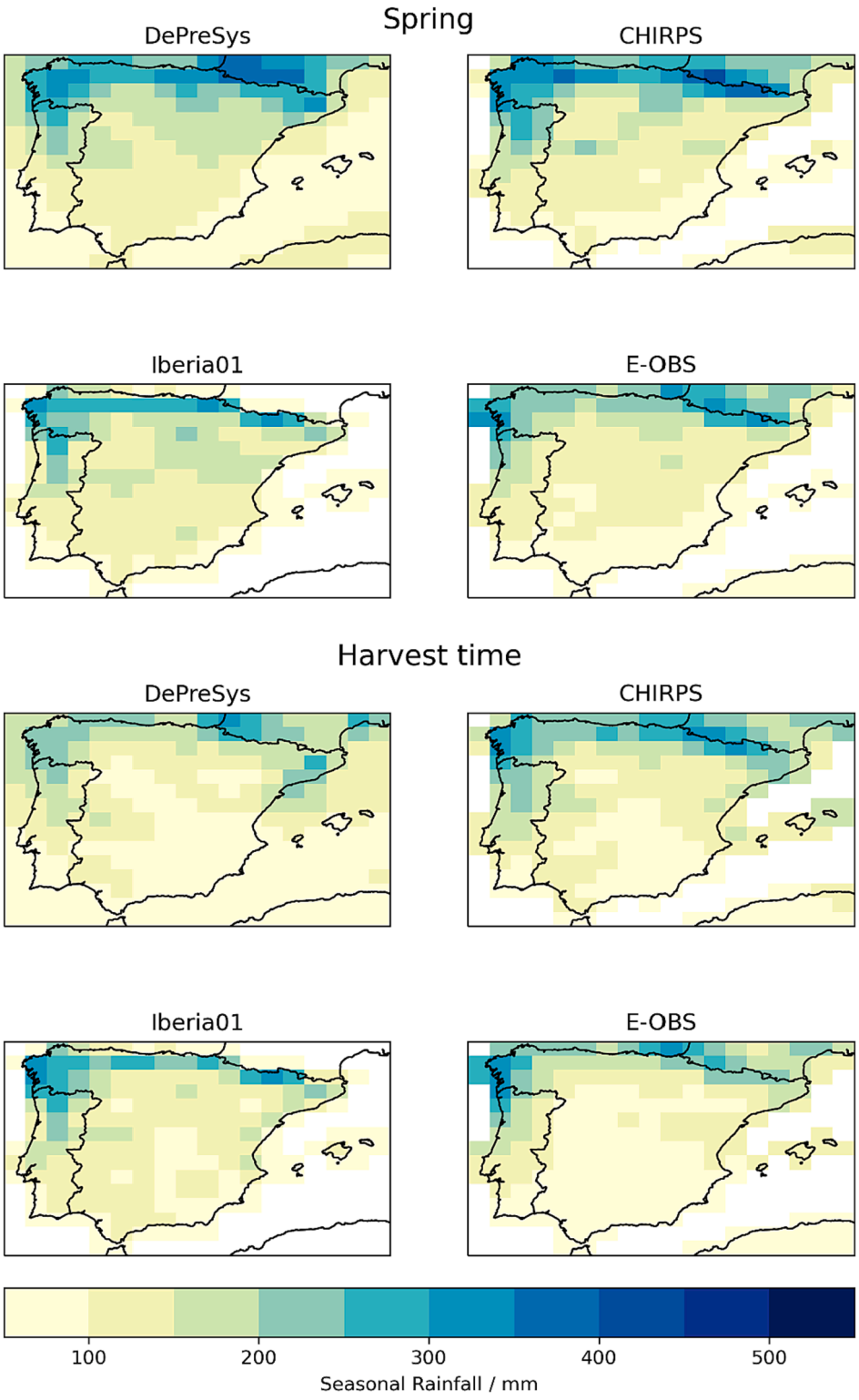

Fig. 4. Mean of spring (April to June) and harvest time (August to October) rainfall totals over the Iberian Peninsula, from DePreSys3 (1980–2017), CHIRPS (1981–2017), Iberia01 (1980–2015) and E-OBS (1980–2017). The DePreSys3 data are an average over all years and ensemble members. The rainfall totals from Iberia01, CHIRPS and E-OBS were aggregated to the resolution of DePreSys3 using an area-weighted method.

range and whiskers from the correlations between the original hindcasts all lie within the 95 % confidence intervals, although the statistics for harvest time lie close to the edges. The permutation test indicates that the DePreSys ensemble members are independent of one another, and therefore contain unique precipitation events.

3.2.3. *Fidelity of the hindcasts*

The fidelity of the DePreSys3 hindcasts is assessed further over the study area of northern Portugal (Fig. 1). A key requirement is that the distribution of rainfall in the model ensemble members and observations should be indistinguishable (Thompson et al., 2017). Time series of rainfall totals over northern Portugal were calculated from the hindcasts

Table 2
Pearson correlation coefficients (R) between the ensemble mean precipitation totals from DePreSys and rainfall totals in spring and harvest time from the three datasets CHIRPS, Iberia01 and E-OBS. The corresponding p-values are shown in parentheses.

Dataset	Spring	Harvest time
CHIRPS	0.08 (0.62)	0.29 (0.08)
Iberia01	0.12 (0.47)	0.31 (0.07)
E-OBS	0.12 (0.47)	0.41 (0.01)

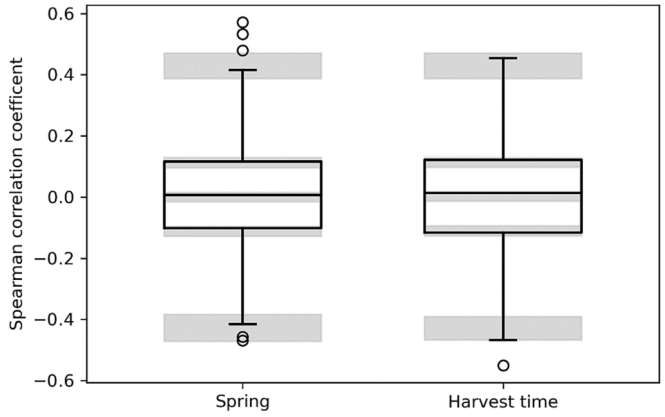

Fig. 5. Boxplots of the 780 Spearman correlation coefficients for spring and harvest time. The box limits indicate the interquartile range, and the centre line shows the median. The whiskers represent 1.5× the interquartile range. Grey shading shows the 95 % confidence intervals of the boxplot statistics estimated from a permutation test consisting of 1000 samples. Outlying data points are shown by open circles.

for spring and harvest time. For each 3-month period, 10,000 proxy time series of length equal to the observations (38 years) were sampled by bootstrapping with replacement from the modelled rainfall series. The modelled and observed rainfall totals are considered indistinguishable if the mean, standard deviation, skewness and kurtosis from the observations are within the central 95 % of the model bootstraps (Thompson et al., 2017; Thompson et al., 2019). For both spring and harvest time, the standard deviation, skewness and kurtosis from all three observed datasets (Iberia01, E-OBS and CHIRPS) lie within this percentile range. For CHIRPS and Iberia01 (Figs. 6, S3 and S4), the mean spring rainfall totals were within the central 95 % of the model bootstraps, but there was a dry bias in the mean of the modelled rainfall for harvest time. For E-OBS, the modelled spring rainfall totals had a wet bias, but the harvest rainfall totals were in good agreement with the modelled values (Fig. S5).

Biases in modelled rainfall amounts are often corrected using methods that modify the entire distribution (Mendez et al., 2020). These methods would therefore change the standard deviation, skewness and kurtosis of the modelled data, which is not desirable in the present study. Instead, biases in the modelled rainfall totals were corrected by applying an additive bias correction method. The ensemble mean bias was calculated, and then this bias was added to all of the hindcast ensemble members. This approach corrects the bias in the mean rainfall totals but has no effect on the other characteristics of the modelled rainfall distribution.

All the observed metrics now lie within the central 95 % of the model distributions (Fig. 6; Supplemental material, Figs. S3–S5); therefore, the model is considered to be statistically indistinguishable from the observations (Thompson et al., 2017; Thompson et al., 2019). Three sets of bias-corrected modelled precipitation totals have been produced, which will be used to estimate the probabilities of unprecedented rainfall totals in spring and harvest time.

3.3. *Unprecedented rainfall events*

The highest observed rainfall totals from all three observational datasets for spring and harvest time are shown in Table 3. The observed rainfall series derived from CHIRPS are reproduced in Fig. 7 (black lines), and the highest observed rainfall totals are indicated by the horizontal dashed lines. The red lines show the rainfall totals from all 40 members of the decadal hindcasts. Similar figures using Iberia01 and E-

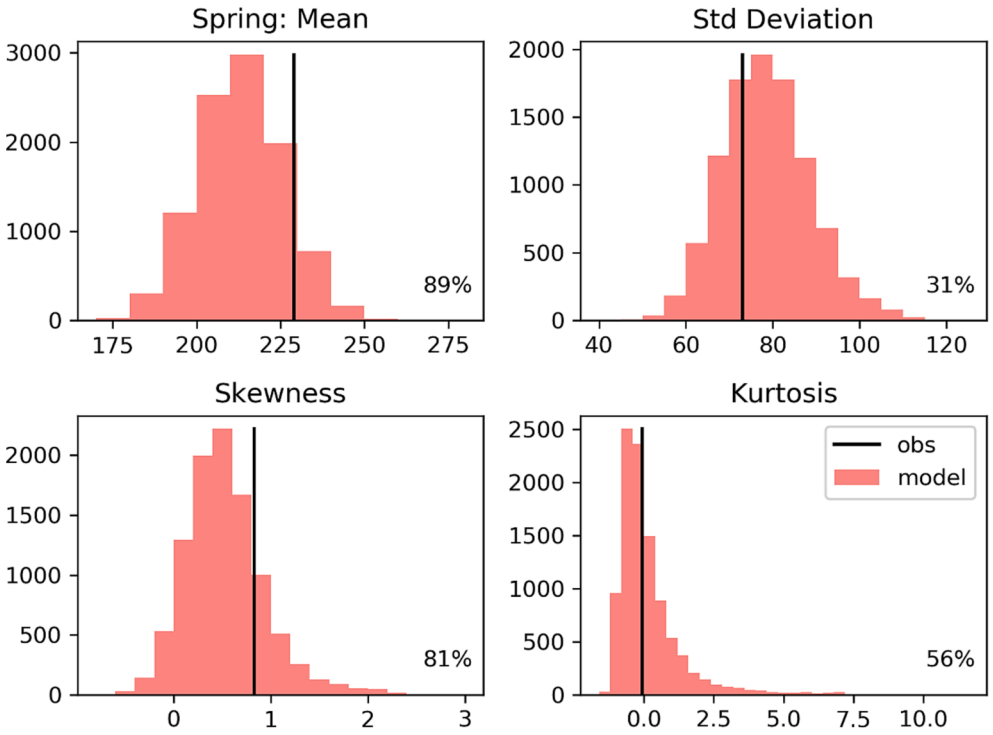

Fig. 6. The distributions of the mean, standard deviation, skewness and kurtosis of the sampled modelled precipitation data (light red) compared with the observed values from CHIRPS (black vertical line) for spring (April to June). The vertical scales indicate the number of values in each of the histogram bins. The percentile of the observed value in the sampled model distribution is shown at the lower right of each panel. Modelled distributions are compared with CHIRPS rainfall totals for harvest time in Fig. S3. (For interpretation of the references to colour in this figure legend, the reader is referred to the web version of this article.)

Table 3
Probabilities of unprecedented rainfall from the decadal hindcasts. The column headings show the observational datasets used to bias-correct the precipitation totals in the hindcasts. The rows "Number above Max" show the number of times that precipitation totals in the hindcasts exceeded the maximum observed value for the given season. The row immediately below shows the corresponding probability and 95% confidence intervals; the latter were calculated using Wilson score intervals. The bottom row shows the numbers of years in the hindcasts with extreme rainfall in both seasons and the estimated probabilities.

	CHIRPS	Iberia01	E-OBS
Spring (April to June)			
Max Observed/mm	418	456	339
Number above Max	20	7	41
Probability (95 % C.I.)	0.013 (0.008, 0.020)	0.005 (0.002, 0.009)	0.027 (0.020, 0.036)
Harvest time (August to September)			
Max Observed/mm	389	460	364
Number above Max	56	13	43
Probability (95 % C.I.)	0.037 (0.028, 0.047)	0.009 (0.005, 0.015)	0.028 (0.021, 0.038)
Number of years in hindcasts with extreme precipitation in both seasons (probability).	18 (0.012)	21 (0.014)	2 (0.001)

OBS are shown in the Supplemental material (Fig. S6). Unprecedented events occur when rainfall totals in the hindcasts exceed the highest observed values. Trends in the numbers and magnitudes of the unprecedented rainfall events in the hindcasts were calculated using a linear regression method that is robust to outliers (Press et al., 1992). Most of the trends were small and close to zero, and none was significant at the 5 % level. The hindcasts include an extremely high rainfall total in each season, over 600 mm in spring and over 700 mm in harvest time. Such events would have a devastating impact on vineyards via severe erosion of soils on the steep slopes and large losses on the vineyards.

From Figs. 7 and S6, the highest observed rainfall totals are exceeded in a small number of years in both seasons (see entries in rows "Number above Max" in Table 3). It is assumed that the unprecedented events occur with probability P, which can be estimated as the number of events divided by the sample size (Kent et al., 2017). A binomial approach is used to estimate the 'counting uncertainty' in these probabilities, using P as the binomial probability of success. The 95 % confidence ranges in these probabilities were estimated using Wilson score intervals (Wilson, 1927). The probability of unprecedented rainfall totals occurring in either season is less than 0.04 (Table 3). The probabilities estimated using the Iberia01 dataset are notably smaller than those estimated with CHIRPS and E-OBS. Results using the CHIRPS and Iberia01 datasets suggest there is a slightly higher probability of unprecedented rainfall totals during harvest time than spring, whereas the probabilities derived using E-OBS are almost the same in both seasons. These results show that the probability of an unprecedented rainfall event over northern Portugal in either season is low. An event might be expected, on average, once in the next 20–100 years in the present climate.

From the observed rainfall data (Fig. S1), both the spring and harvest time were exceptionally wet in 1993. In CHIRPS and E-OBS, the precipitation totals for spring and harvest time of 1993 were almost the same, at 300 mm and 362 mm respectively. The totals in Iberia01 were higher, at 358 mm and 450 mm. Years similar to 1993 were searched for in the hindcasts, using thresholds of 300 mm and 360 mm for either season. The numbers of years with extreme precipitation totals in both seasons vary depending on the dataset used to bias-correct the hindcast data, and are shown in the bottom row of Table 3. The numbers of years were 18 (CHIRPS), 21 (Iberia01) and 2 (E-OBS). E-OBS has a dry bias compared with the other two datasets (Section 3.2.1), so the number of years is correspondingly smaller. The probabilities are 0.012 and 0.014 from modelled data corrected by CHIRPS and Iberia01 respectively. A year similar to 1993 reoccurring in the present climate would be expected to occur, on average, once in the next 70–80 years in the current climate. Although the probability of another year like 1993 is low, it would have a high impact on wine production, via erosion of soils and terraces, damage to the vines and reduced must production.

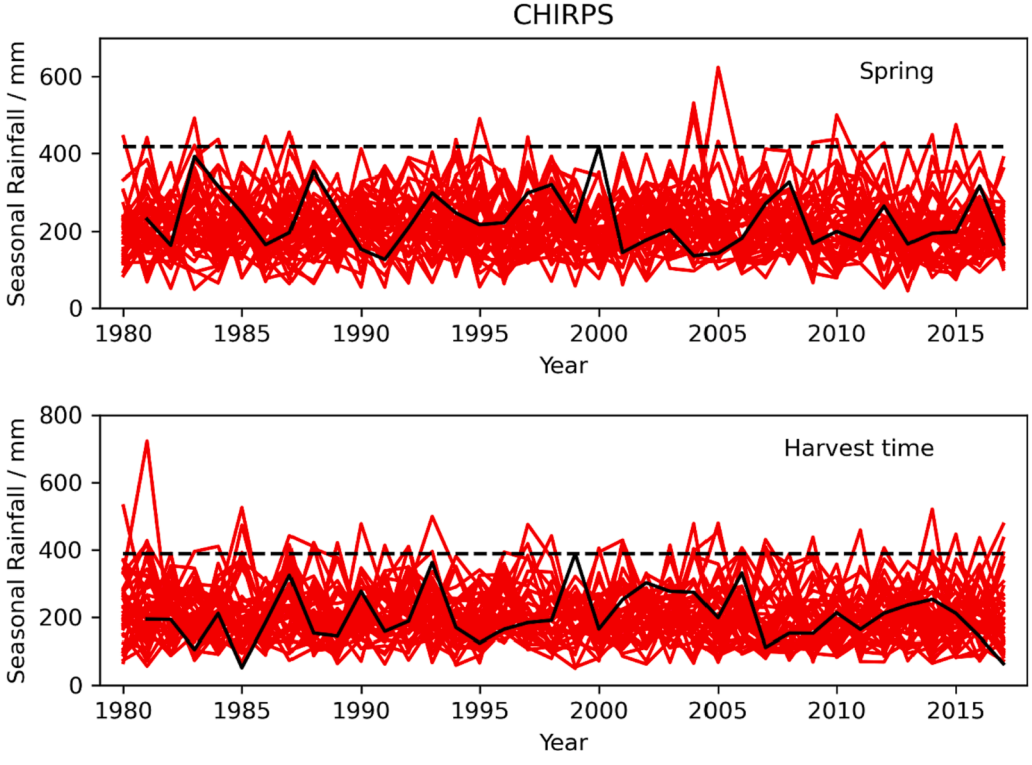

Fig. 7. Unprecedented seasonal rainfall totals for spring (April to June) and harvest time (April to October) in northern Portugal from 1980 to 2017. The solid black lines show observed rainfall totals from CHIRPS (Funk et al., 2015), and the dashed black lines indicate the highest observed values. The red lines represent rainfall totals from the bias-corrected hindcasts (40 members). Unprecedented rainfall totals are apparent when the modelled rainfall totals lie above the dashed line in each panel. (For interpretation of the references to colour in this figure legend, the reader is referred to the web version of this article.)

3.4. Extreme value analysis

Before fitting the Generalised Pareto (GP) model to the data (Section 2.3), it is first necessary to select a suitable threshold u, which must be sufficiently high in order that the values above the threshold can be represented by a GP distribution. However, if the threshold is too high, the model fit becomes unstable because there are too few data points to constrain the GP model. The approach adopted in the present study was to choose the lowest valid threshold (Gilleland and Katz, 2016). The thresholds for each season were identified via inspection of mean residual life (MRL) and threshold choice (TC) plots (Coles, 2001). The "extRemes" package (Gilleland and Katz, 2016) includes functions to create these plots. Examples are shown in the Supplemental material, Fig. S7. In the MRL plot, the mean of the excesses ($x - u$) above a threshold u are plotted as a function of the threshold. The range of appropriate threshold values appears as an approximately linear region (Coles, 2001). In the TC plots, the reparametrized scale parameter $\sigma^* = \sigma_u - \xi u$ and shape parameter ξ are plotted as a function of the threshold. Both parameters should have near-constant values over the range of valid thresholds. In Fig. S7, an approximately linear section is seen in the MRL plot for thresholds between 250 and 320 mm. The reparametrized scale and shape parameters have near-constant values over the same range, so that a threshold of 250 mm was chosen for spring. The GP thresholds for both seasons using hindcast data bias-corrected with each of the observed datasets (Section 3.2.3) are listed in Table 4.

Some of the MRL and TC plots created using the observed rainfall totals were harder to interpret, and suitable thresholds could not be easily identified. For all datasets (modelled and observed), the GP model was repeatedly fitted to the data using a range of thresholds, starting at 100 mm and increasing in steps of 10 mm. Diagnostic plots produced by "extRemes", showing quantile–quantile comparisons and histograms of rainfall totals from the data and fitted GP model, allowed the quality of the fit to be assessed (see Coles (2001), pp. 88–89, and "Fig. 2″ of Gilleland and Katz (2016)). Thresholds chosen from the MRL and TC plots (Table 4) were further verified using the best fit of the GP model to the observed or modelled data as inferred from the diagnostic plots.

The magnitudes of rainfall totals for each season are shown against their return periods in Figs. 8 and S8. It is apparent that the confidence intervals associated with the observed data (green dashed lines) are much wider than those of the modelled data (grey dashed lines). There are larger numbers of extreme events in the decadal hindcasts with which to constrain the GP model. The return level curves in Figs. 8 and S8 show that the use of a large ensemble of model simulations means the uncertainties in the return levels are greatly constrained compared with using the observations. The return levels for longer return periods are generally higher in the modelled data than the observed, particularly in harvest time. However, the confidence intervals of the observed data contains the modelled curves for all time periods, showing that both the modelled and observed extremes come from the same distribution.

The probabilities of exceeding the highest observed values in each dataset were calculated from the parameters of the GP curves fitted to the modelled data, and are shown in Table 4. These probabilities are in good agreement with those estimated from the decadal hindcasts in Section 3.3, and the 95 % confidence intervals overlap. In most cases, the probabilities of unprecedented rainfall totals calculated from the fit of the GP model to the hindcasts are slightly higher than those estimated directly from the decadal hindcasts.

Table 4
Maximum observed rainfall totals and probabilities of unprecedented rainfall totals estimated from the decadal hindcasts and GP distributions. The 95% confidence intervals (C.I.) are shown in parentheses after the probabilities. Where necessary, the mean of the modelled precipitation totals was adjusted to equal the mean of the given observed dataset as described in Section 3.2. The GP thresholds will therefore depend on the observed dataset used for the bias correction.

	CHIRPS	Iberia01	E-OBS
Spring (April–June)			
Max Observed/mm	418	456	339
GP Threshold (mm)	240	250	200
GP Probability (95 % C.I.)	0.016 (0.011, 0.021)	0.007 (0.003, 0.010)	0.029 (0.022, 0.036)
Hindcast Probability (95 % C.I.)	0.013 (0.008, 0.020)	0.005 (0.002, 0.009)	0.027 (0.020, 0.036)
Harvest time (August to September)			
Max Observed/mm	389	460	364
GP Threshold (mm)	160	220	200
GP Probability (95 % C.I.)	0.042 (0.034, 0.050)	0.013 (0.009, 0.018)	0.022 (0.015, 0.026)
Hindcast Probability (95 % C.I.)	0.037 (0.029, 0.048)	0.009 (0.005, 0.015)	0.028 (0.021, 0.038)

4. Discussion

Heavy rainfall can cause severe disruption to vine growers in northern Portugal and result in economic losses. High rainfall during spring (April to June) can promote growth of the vines but increases the risk of fungal disease. Heavy rainfall during harvest time (August to October) can reduce the quality of the grapes, promote fungal outbreaks, reduce overall yields and has the potential for severe operational disruption during harvesting. An understanding of the risk of unprecedented rainfall totals is therefore of interest to wine producers. A large ensemble of decadal hindcasts has been used to estimate the probability of unprecedented rainfall events over northern Portugal in the current climate. The large ensemble of model simulations, with nearly-two orders of magnitude more data than the observational record, allows the probability and return periods of extreme monthly rainfall to be estimated robustly.

Unprecedented rainfall totals are possible under the current climate in northern Portugal during spring and harvest time. The probability of an unprecedented rainfall event in each season was estimated from the hindcasts by counting the number of events with rainfall totals higher than the maximum observed values. The probability in both seasons was less than 0.04. A complementary analysis using extreme value theory provided estimated probabilities that were slightly higher, although the 95 % confidence intervals of the probabilities overlap. An unprecedented rainfall event might be expected, on average, just once in each season over the next 20–100 years. Further analysis of the hindcasts showed that the probability of reoccurrence of another year similar to 1993, with very high rainfall in both spring and harvest time, is also low, and might occur, on average, once in the next 70–80 years in the current climate. Nevertheless, a year similar to 1993 could have high negative impacts on the area, via erosion of the terraces, loss of vines and reduced must production. The decadal hindcast ensemble is based on a dynamical model of the atmosphere and ocean (Williams et al., 2015), giving confidence that such unprecedented rainfall events could happen physically, and are not just the result of statistical extrapolation.

As well as quantifying the probability of unprecedented events, the DePreSys3 hindcast has also revealed a remarkably high rainfall extreme in each season: spring $>$ 600 mm and harvest time $>$ 700 mm. Although both of these events have a very low probability of occurrence (less than 1 in 1,000 years), some users might be interested that such large extremes might occur in the current climate. Such events could have a devastating impact on vineyards due to erosion of soils on the steep slopes, depending upon the spatiotemporal pattern of the rainfall within that season. The hindcasts used in the present study consisted of 40 ensemble members produced from the same climate model. In order to account for model structural error, ensembles from other near-term prediction systems could be used in the future (Jain et al., 2020), which would also increase the size of the sample of unprecedented rainfall events for study.

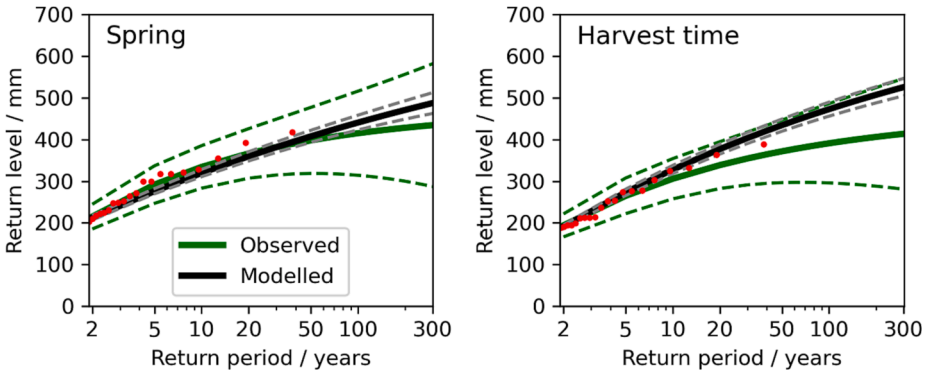

Fig. 8. Return level curves from fitting a Generalised Pareto (GP) extreme value distribution to seasonal rainfall totals in the CHIRPS dataset (green lines) and decadal hindcasts (black lines) above the thresholds given in Table 4. Curves are shown for spring (April to June) and harvest time (August to October). Solid red circles represent empirical return levels for the observed rainfall totals. The solid lines show the fitted GP curves and the dashed lines the 95% confidence intervals. (For interpretation of the references to colour in this figure legend, the reader is referred to the web version of this article.)

Few studies have assessed the skill of seasonal and decadal forecasts for northern Portugal. Santos et al. (2020) developed a statistical model of port wine production for the Douro and Porto DOC region, which was combined with seasonal forecasts to predict wine production. An extension of the work presented here would be to assess seasonal forecast skill of unprecedented rainfall amounts in spring and harvest time. If the forecast model is skilful, a service could be provided to wine growers in northern Portugal. Other studies have improved seasonal forecast skill of extreme precipitation using machine learning (Civitarese et al., 2021).

Other data sources could be used to estimate the probability of rare and unprecedented climatic events. Gessner et al. (2021) applied statistical methods to a very long (about 5000 year) global climate model simulation to estimate the magnitudes of unprecedented heat extremes. A similar approach could be used to study unprecedented rainfall totals. Weather generators, which are stochastic models trained on observations, have been used to simulate numbers and magnitudes of climate extremes (Gitau et al., 2018; Nguyen et al., 2021). Some weather generators are capable of simulating unprecedented climatic events, such as low and high rainfall scenarios more extreme than those observed (Serinaldi and Kilsby, 2012).

This study has focused on two metrics, which are the total rainfall amounts over northern Portugal for spring and harvest time. One extension to this study would be to consider the numbers and timing of heavy rainfall events. Heavy rain in spring 2016 mostly occurred on three days (Fig. S2), two of which were only 4 days apart. In other years, the rainfall could be spread over a larger number of days and occur in different parts of the season which could moderate the exact impacts on wine production. The probabilities of other climatic extremes could also be evaluated. Heat waves during the viticultural cycle can also reduce yields; the European heat wave and drought of 2022 is expected to reduce yields in several countries, including Portugal (OIV, 2022b). The model simulations also allow investigation into the circulation patterns and causes of extreme events, but such an analysis is beyond the scope of the present study. In the study area, vines are the major crop type, but almonds and olives are also grown. The same approach used here could be tailored to calculate the probabilities of unprecedented rainfall in key seasons for other crop types.

This study is the first to assess the probability of unprecedented rainfall extremes over northern Portugal. The probability of heavy rainfall in spring and harvest time in the present climate is low (0.01 to 0.05), and the probability of a year similar to 1993 with heavy rainfall in both seasons is also small. Nevertheless, the impact of heavy rainfall in either or both seasons could be high, including damage to vines and reduced production. These results help inform the need for and size of costly adaptation investments, such as better availability of spraying machinery and labour, high-gauge drainage, landslide controls or even abandonment of exposed vineyard areas.

CRediT authorship contribution statement

Michael G. Sanderson: Conceptualization, Formal analysis, Funding acquisition, Methodology, Software, Visualization, Writing – original draft, Writing – review & editing. **Marta Teixeira:** Conceptualization, Data curation, Project administration, Validation, Writing – original draft, Writing – review & editing. **Natacha Fontes:** Data curation, Writing – original draft. **Sara Silva:** Data curation, Writing – original draft. **António Graça:** Conceptualization, Data curation, Funding acquisition, Methodology, Project administration, Validation, Writing – original draft, Writing – review & editing.

Declaration of Competing Interest

The authors declare that they have no known competing financial interests or personal relationships that could have appeared to influence the work reported in this paper.

Data availability

A Data Sources section showing links to all the data used is at the end of the supplemental material.

Acknowledgements

This research was supported by the project MED-GOLD (Turning climate-related information into added value for traditional MEDiterranean Grape, OLive and Durum wheat food systems) through the European Union's Horizon 2020 research and innovation programme [grant agreement No. 776467]. The authors acknowledge the E-OBS dataset from the EU-FP6 project UERRA (http://www.uerra.eu) and the Copernicus Climate Change Service, and the data providers in the ECA&D project (https://www.ecad.eu). The authors thank António Seabra from DRAP-N and Maria do Carmo Val from ADVID for data provided. Also, Nick Dunstone for helpful comments on an earlier version of the manuscript.

Appendix A. Supplementary data

Supplementary data to this article can be found online at https://doi.org/10.1016/j.cliser.2023.100363.

References

ADVID, 2016. Boletim Informativo 13-2016. (https://www.advid.pt).
Alcoforado, M.J., Silva, L.P., Amorim, I., Fragoso, M., Garcia, J.C., 2021. Historical floods of the Douro River in Porto, Portugal (1727–1799). Clim. Change 165, 17. https://doi.org/10.1007/s10584-021-03039-7.
Alves, F., Valente, J., Carvalho, J., & Bateira, C. (2021). Sustainable Viticulture: Reviewing the terraces geometry in the Douro Region. Guidelines to growers and policymakers. In Atas do Congresso Douro e Porto: Memória com Futuro. https://hdl.handle.net/10216/136620.

Civitarese, D. S., Szwarcman, D., Zadrozny, B., & Watson, C. (2021). Extreme Precipitation Seasonal Forecast Using a Transformer Neural Network. Paper #44, presented at the ICML 2021 Workshop: Tackling Climate Change with Machine Learning. https://www.climatechange.ai/papers/icml2021/44.

Coles, S., 2001. An Introduction to Statistical Modeling of Extreme Values. Springer-Verlag, London and Berlin.

Cornes, R., van der Schrier, G., van den Besselaar, E.J.M., Jones, P.D., 2018. An ensemble version of the E-OBS temperature and precipitation datasets. J. Geophys. Res. Atmos. 123, 9391–9409. https://doi.org/10.1029/2017JD028200.

Cui, D., Liang, S., Wang, D., Liu, Z., 2021a. A 1-km global dataset of historical (1979–2017) and future (2020–2100) Köppen-Geiger climate classification and bioclimatic variables. Earth Sys. Sci. Data 13, 5087–5114. https://doi.org/10.5194/essd-13-5087-2021.

Cui, D., Liang, S., Wang, D., Liu, Z., 2021b. KGClim historical: A 1-km global dataset of historical (1979–2013) Köppen-Geiger climate classification and bioclimatic variables (Version V2). Zenodo. https://doi.org/10.5281/zenodo.5347837.

Cunha, S., Silva, Á., Herráez, C., Pires, V., Chazarra, A., Mestre, A., Nunes, L., Mendes, M., Neto, J., Marques, J., & Mendes, L. (2011). Atlas Climático Ibérico. ISBN: 978-84-7837-079-5. https://www.ipma.pt/en/publicacoes/clima/index.jsp?page=atlas.clima.xml.

Dunstone, N., Smith, D., Scaife, A., Hermanson, L., Eade, R., Robinson, N., Andrews, M., Knight, J., 2016. Skilful predictions of the winter North Atlantic Oscillation one year ahead. Nat. Geosci. 9, 809–814. https://doi.org/10.1038/ngeo2824.

Faria, A., Bateira, C., Oliveira, S., Fernandes, J., Marques, F., 2017. Landslide susceptibility evaluation on agricultural terraces by the application of physically based mathematical models. Revista do Departamento de Geografia 33, 1–11. https://doi.org/10.11606/rdg.v33i0.122883.

Fernandes, J., Bateira, C., Soares, L., Faria, A., Oliveira, A., Hermenegildo, C., Moura, R., Gonçalves, J., 2017. SIMWE model application on susceptibility analysis to bank gully erosion in Alto Douro Wine Region agricultural terraces. Catena 153, 39–49. https://doi.org/10.1016/j.catena.2017.01.034.

Fonseca, S., Rebelo, J., 2010. Economic valuation of cultural heritage: application to a museum located in the Alto Douro Wine Region-World Heritage Site. PASOS Revista de turismo y patrimonio cultural 8 (2), 339–350. https://doi.org/10.25145/j.pasos.2010.08.024.

Fraga, H., de Cortázar, G., Atauri, I., Malheiro, A.C., Moutinho-Pereira, J., Santos, J.A., 2017. Viticulture in Portugal: A review of recent trends and climate change projections. OENO One 51, 61–69. https://doi.org/10.20870/oeno-one.2017.51.2.1621.

Funk, C., Peterson, P., Landsfeld, M., Pedreros, D., Verdin, J., Shukla, S., Husak, G., Rowland, J., Harrison, L., Hoell, A., Michaelsen, J., 2015. The climate hazards infrared precipitation with stations - a new environmental record for monitoring extremes. Sci. Data 2, 150066. https://doi.org/10.1038/sdata.2015.66.

Gessner, C., Fischer, E.M., Beyerle, U., Knutti, R., 2021. Very rare heat extremes: Quantifying and understanding using ensemble reinitialization. J. Clim. 34, 6619–6634. https://doi.org/10.1175/JCLI-D-20-0916.1.

Gilleland, E., Katz, R.W., 2016. extRemes 2.0: An Extreme Value Analysis Package in R. J. Stat. Softw. 72 https://doi.org/10.18637/jss.v072.i08.

Gitau, M.W., Mehan, S., Guo, T., 2018. Weather generator effectiveness in capturing climate extremes. Environ. Process. 5 (Suppl 1), 153–165. https://doi.org/10.1007/s40710-018-0291-x.

Gladstones, J., 2011. Wine, terroir and climate change. Wakefield Press, Kent Town, Australia.

Hénin, R., Ramos, A.M., Pinto, J.Q., Liberato, M.L.R., 2021. A ranking of concurrent precipitation and wind events for the Iberian Peninsula. Int. J. Climatol. 41, 1421–1437. https://doi.org/10.1002/joc.6829.

Herrera, S., Cardoso, R.M., Soares, P.M., Espírito-Santo, F., Viterbo, P., Gutiérrez, J.M., 2019. Iberia01: a new gridded dataset of daily precipitation and temperatures over Iberia. Earth Syst. Sci. Data 11, 1947–1956. https://doi.org/10.5194/essd-11-1947-2019.

Herrera, S., Cardoso, R. M., Soares, P. M., Espírio-Santo, F., Viterbo, P., & Gutiérrez, J. M. (2019b). Iberia01: Daily gridded (0.1° resolution) dataset of precipitation and temperatures over the Iberian Peninsula. ; DIGITAL.CSIC; https://doi.org/10.20350/digitalCSIC/8641.

Jain, S., Scaife, A. A., Dunstone, N., Smith, D., & Mishra, S. K. (2020). Current chance of unprecedented monsoon rainfall over India using dynamical ensemble simulations. Environ. Res. Lett., 15, 094095, https://doi.org/10.1088/1748-9326/ab7b98.

Jones, G.V., Alves, F., 2012. Impact of climate change on wine production: a global overview and regional assessment in the Douro Valley of Portugal. Int. J. Glob. Warming 4, 383–406. https://doi.org/10.1504/IJGW.2012.049448.

Kelder, T., Müller, M., Slater, L.J., Marjoribanks, T.I., Wilby, R.L., Prudhomme, C., Bohlinger, P., Ferranti, L., Nipen, T., 2020. Using UNSEEN trends to detect decadal changes in 100-year precipitation extremes. NPJ Clim. Atmos. Sci. 3, 47. https://doi.org/10.1038/s41612-020-00149-4.

Kelder, T., Marjoribanks, T.I., Slater, L.J., Prudhomme, C., Wilby, R.L., Wagemann, J., Dunstone, N., 2022. An open workflow to gain insights about low-likelihood high-impact weather events from initialized predictions. Meteorol. Appl. 29, e2065.

Kent, C. K., Pope, E., Thompson, V., Lewis, K., Scaife, A. A., & Dunstone, N. (2017). Using climate model simulations to assess the current climate risk to maize production. Environ. Res. Lett., 12, 054012, doi:10.1088/1748-9326/aa6cb9.

Martins, J., Fraga, H., Fonseca, A., Santos, J.A., 2021. Climate projections for precipitation and temperature indicators in the Douro wine region: The importance of bias correction. Agronomy 11, 990. https://doi.org/10.3390/agronomy11050990.

Mendez, M., Maathuis, B., Hein-Griggs, D., Alvarado-Gamboa, L.-F., 2020. Performance evaluation of bias correction methods for climate change monthly precipitation projections over Costa Rica. Water 12, 482. https://doi.org/10.3390/w12020482.

Millar, R. (2018). Violent storms batter heart of the Douro, https://www.thedrinksbusiness.com/2018/05/violent-storms-batter-heart-of-the-douro/.

Nguyen, V.D., Merz, B., Hundecha, Y., Haberlandt, U., Vorogushyn, S., 2021. Comprehensive evaluation of an improved large-scale multi-site weather generator for Germany. Int. J. Climatol. 41, 4933–4956. https://doi.org/10.1002/joc.7107.

OIV (2010). Resolution OIV/VITI 333/2010. https://www.oiv.int/public/medias/382/viti-2010-1-fr.pdf.

OIV (2022a). State of the world vine and wine sector 2021: April 2022. International Organisation of Vine and Wine, Paris, France. (https://www.oiv.int).

OIV (2022b). World Wine Production Outlook: OIV First Estimates, 31.10.2022. https://www.oiv.int/press/severe-drought-and-extreme-heat-pose-new-threat-wine-production.

Owen, L. E., Catto, J. L., Dunstone, N. J, & Stephenson, D. B. (2021). How well can a seasonal forecast system represent three hourly compound wind and precipitation extremes over Europe? Environ. Res. Lett., 16, 074019, https://doi.org/10.1088/1748-9326/ac092e.

Press, W.H., Teukolsky, S.A., Vetterling, W.T., Flannery, B.P., 1992. Numerical Recipes in Fortran 77: The Art of Scientific Computing, second Ed. Cambridge University Press, Cambridge, UK.

Santos, J.A., Ceglar, A., Toreti, A., Prodhomme, C., 2020. Performance of seasonal forecasts of Douro and Port wine production. Agric. For. Meteorol. 291, 108095 https://doi.org/10.1016/j.agrformet.2020.108095.

Santos, M., Santos, J.A., Fragoso, M., 2015. Historical damaging flood records for 1871–2011 in Northern Portugal and underlying atmospheric forcings. J. Hydrol. 530, 591–603. https://doi.org/10.1016/j.jhydrol.2015.10.011.

Serinaldi, F., Kilsby, C.G., 2012. A modular class of multisite monthly rainfall generators for water resource management and impact studies. J. Hydrol. 464–465, 528–540. https://doi.org/10.1016/j.jhydrol.2012.07.043.

Thompson, V., Dunstone, N., Scaife, A., Smith, D., Slingo, J., Brown, S., Belcher, S., 2017. High risk of unprecedented UK rainfall in the current climate. Nat. Commun. 8, 107. https://doi.org/10.1038/s41467-017-00275-3.

Thompson, V., Dunstone, N., Scaife, A.A., Smith, D.M., Hardiman, S.C., Ren, H.-L., Lu, B., Belcher, S.E., 2019. Risk and dynamics of unprecedented hot months in South East China. Clim. Dyn. 52, 2585–2596. https://doi.org/10.1007/s00382-018-4281-5.

Williams, K.D., Harris, C.M., Bodas-Salcedo, A., Camp, J., Comer, R.E., Copsey, D., Fereday, D., Graham, T., Hill, R., Hinton, T., Hyder, P., Ineson, S., Masato, G., Milton, S.F., Roberts, M.J., Rowell, D.P., Sanchez, C., Shelly, A., Sinha, B., Walters, D.N., West, A., Woollings, T., Xavier, P.K., 2015. The Met Office Global Coupled model 2.0 (GC2) configuration. Geosci. Model Dev. 8, 1509–1524. https://doi.org/10.5194/gmd-8-1509-2015.

Wilson, E.B., 1927. Probable inference, the law of succession, and statistical inference. J. Am. Stat. Assoc. 22, 209–212. https://doi.org/10.1080/01621459.1927.10502953.

Zhu, J., Frayssse, R., Trought, M.C.T., Raw, V., Yang, L., Greven, M., Martin, D., Agnew, R., 2020. Quantifying the seasonal variations in grapevine yield components based on pre- and post-flowering weather conditions. OENO One 54 (2). https://doi.org/10.20870/oeno-one.2020.54.2.2926.